Journal of Photochemistry and Photobiology A: Chemistry 218 (2011) 11–16

Contents lists available at ScienceDirect

Journal of Photochemistry and Photobiology A: Chemistry

journal homepage: www.elsevier.com/locate/jphotochem

Picosecond deactivation of azo dye excited states in solution and in cellulose

Laurence C. Abbott[a], Stephen N. Batchelor[b,*], Lisinka Jansen[b], John Oakes[b], John R. Lindsay Smith[a], John N. Moore[a,*]

[a] Department of Chemistry, The University of York, Heslington, York YO10 5DD, UK
[b] Unilever Research, Port Sunlight, Quarry Road East, Bebington, Wirral CH63 3JW, UK

ARTICLE INFO

Article history:
Received 12 June 2010
Received in revised form
15 November 2010
Accepted 25 November 2010
Available online 2 December 2010

Keywords:
Azo dye
Picosecond
Time-resolved UV–visible spectroscopy
Cellulose
Cellophane

ABSTRACT

Ultrafast time-resolved UV–visible absorption spectroscopy has been used to study four model azo dyes and five commercial azo dyes. All of the dyes have been found to show strong bleaching of their ground-state absorption bands on photoexcitation, with recovery lifetimes of 1–5 ps in aqueous solution that are attributed to rapid and efficient non-radiative decay; two commercial azo dyes deposited in cellophane have been found to show an additional longer-lived component with a lifetime of >50 ps that is attributed to the effects of intermolecular interactions with the cellulosic environment.

1. Introduction

Azo dyes are the largest class of industrial dyes, and they are used in a wide range of applications such as textiles, printing, food additives, and pharmaceuticals. The photofading of azo dyes generally occurs with very low quantum yield but it can become significant over the life-span of dyed products, and many dyes photofade more rapidly on surfaces than they do in solution by complex mechanisms whose details are not fully understood [1–4]. The routes and yields of photochemical reactions are determined at the outset by primary excited-state behaviour, and information on the dynamics of the excited states of azo dyes in solution and on surfaces is required to develop a detailed understanding of their photochemistry.

The relatively simple azobenzene molecule undergoes *trans–cis* photoisomerisation on excitation, and our initial time-resolved studies of the ultrafast dynamics [5–7] have led to extensive studies and discussions of the precise mechanisms [8–11]. Commercial azo dyes have more complicated structures than azobenzene, and many have hydroxylated structures based on arylazonaphthols [12], with the hydrazone tautomer commonly being dominant over the azo tautomer depending on the dye structure and conditions such as solvent and temperature. A variety of nanosecond and longer time-resolved studies of azo/hydrazone dyes have been described, including studies of their photochemical production of singlet oxygen in low yield [13,14] and their thermal reactions with various species including short-lived radicals produced by photolysis or radiolysis [15–21], but comparatively few direct studies of the excited states or ultrafast dynamics of azo/hydrazone dyes have been reported. Picosecond UV–visible absorption studies of the monoazo dye Orange II (Acid Orange 7) and the bisazo dye Naphthol Blue Black (Acid Black 1) in alcohols gave time-resolved spectra dominated by ground-state bleaching that showed transient loss of the ground-state UV–visible absorption band with recovery lifetimes of ca. 100 and 30 ps, respectively [22,23]. More recent emission [24] and transient lens [25] studies of Orange II gave solvent-dependent excited state lifetimes of ca. 1–10 ps that increased to ca. ≤200 ps on cyclodextrin or protein binding. Other mono- and bisazo dyes gave emission and bleach-recovery lifetimes of ca. 1–3 ps in solution [26], and a novel set of fluorenone-bisazo dyes gave transient absorption and bleach-recovery lifetimes of ca. 10–500 ps in non-aqueous solutions, with the hydrazone tautomers having longer lifetimes than the azo tautomers [27].

We have been carrying out detailed studies of model and commercial azo/hydrazone dyes using a variety of spectroscopic and computational techniques in order to understand their structures in solution and in cellulosic environments, including their tautomer, aggregation and protonation states [28–30]. We have also studied the structure of short-lived dye radicals generated in high yield by reduction with 2-hydroxy-2-propyl radicals produced

* Corresponding authors. Tel.: +44 1904 322548; fax: +44 1904 322516.
E-mail addresses: john.moore@york.ac.uk (J.N. Moore), Stephen.Batchelor@unilever.com (S.N. Batchelor).

1010-6030/$ – see front matter © 2011 Elsevier B.V. All rights reserved.
doi:10.1016/j.jphotochem.2010.11.017

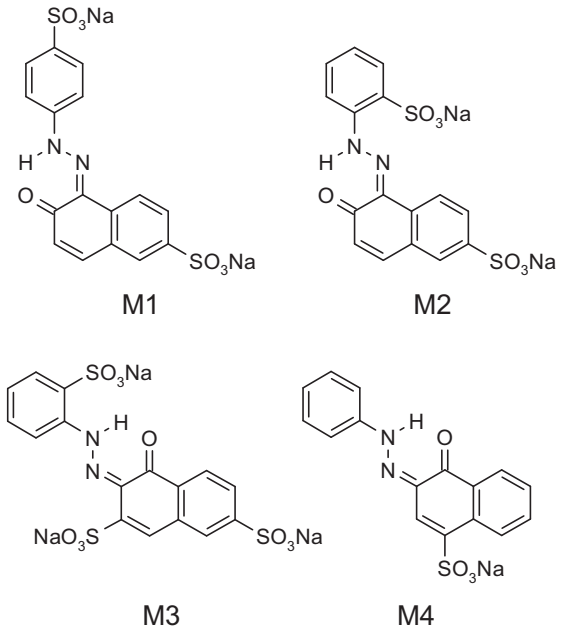

Fig. 1. Structures of the four model dyes.

chemically or photochemically from other reagents, and their radical reaction mechanisms from nanoseconds through to products [31,32]. Our steady-state studies of the direct photochemistry of azo/hydrazone dyes in the absence of radical-producing reagents have indicated that they typically have very low photodegradation reaction yields [32] which are slightly higher in cellulose than in solution [2]. Hence, there is a need for time-resolved studies to make direct observations of the underlying excited state dynamics of azo/hydrazone dyes, both in solution and on the cellulose surfaces in which they find their widest commercial applications.

Here, we report ultrafast time-resolved UV–visible (TRVIS) studies of four model and five commercial azo dyes in aqueous solution and of two commercial dyes deposited in cellophane, which is a transparent cellulosic material that we have shown to be a good mimic of cotton [2,28]. The four monoazo dyes we have studied are shown in Fig. 1, and they were chosen as simple models for the widely used 1-phenylazo-2-naphthol and 2-phenylazo-1-naphthol groups present within many commercial azo dyes [33]; they commonly occur in the hydrazone form, as shown in Fig. 1, and the sulfonate groups provide good water solubility. The five commercial dyes we have studied are examples of black and blue dyes from reactive and direct classes [12] that are widely used to dye cellulosic textiles such as cotton and viscose; they were chosen because cotton is the most widely used clothing fabric, and because black and blue are the most common colours. The three commercial dyes with structures shown in Fig. 2 have at least one sulfonated 2-arylazo-1-naphthol group, with Direct Blue 1 (Chicago Sky Blue 6B) and Reactive Black 5 (Remazol Black B) being bis-azo dyes, and Direct Blue 71 being a tris-azo dye. We have also studied Procion Navy H-EXL (N-HEXL), a commercial monochlorotriazene reactive dye, and Remazol Navy Blue GG (NB-GG), a commercial vinylsulfone reactive dye; their exact structures are not publicly available, but both are understood to contain multiple azo and/or hydrazone groups.

2. Experimental

2.1. Samples

Solid samples of the model and commercial dyes were supplied by Unilever, and were used as received; the synthesis of the model dyes has been reported [33]. Solution samples were prepared using deionised water, and at concentrations of ca. $1–8 \times 10^{-4}$ mol dm^{-3} adjusted to give an absorbance of ca. 0.6–0.7 in a 1-mm pathlength cell at the TRVIS laser excitation wavelength. Cellophane samples were prepared by soaking small (ca. 1 cm × 2 cm) pieces of cellophane film (Sigma, thickness ca. 45 μm) in a dye solution (typically ca. $1–5 \times 10^{-3}$ mol dm^{-3}) for ca. 30 min, and then drying the dyed films between lint-free tissues with weights on top to prevent wrinkling. The concentrations of the dyes in cellophane were estimated by assuming that the peak absorption coefficients were the same as those in solution. All samples were studied at room temperature (ca. 20 °C).

2.2. Steady-state studies

Steady-state UV–visible absorption spectra were recorded using a dual-beam UV–visible spectrometer (Hitachi U-3000). Spectra of solutions were recorded using matched 1-mm pathlength quartz sample and solvent reference cells. Spectra of cellophane films were recorded with the ca. 45-μm pathlength sample held between quartz windows, and with a non-dyed cellophane film as reference.

2.3. Time-resolved studies

The ultrafast laser apparatus and methods for the TRVIS studies have been described in detail previously [5,34]. Briefly, an amplified dye laser system provided pulsed output with a wavelength of 606 nm, pulsewidth of ca. 400 fs, and repetition rate of 1050 Hz, and it was split into two beams. One beam was used to pump the sample either in the visible region (606 nm, pulse energy ca. 3 μJ) or in the UV region after frequency doubling in a BBO crystal (303 nm, pulse energy ca. 1 μJ). The second beam was directed around a variable optical delay line and focused into a cell of D_2O/H_2O to generate a white light continuum which was then used to probe the sample. The probe beam was passed through the sample cell coincident with the pump beam, using near-collinear geometry and with the relative polarisations of the two beams set to the "magic angle" of 54.7°. The transmitted probe beam was analysed using 10-nm band-pass filters, and detected using a photodiode. The pump beam was chopped at 525 Hz using a synchronised mechanical chopper, and two lock-in amplifiers were used to recover the average and differential transmitted probe beam intensities, from which the change in absorbance was calculated. Kinetic traces were fitted by single-exponential or multi-exponential decays convoluted with the instrument response function.

Solution samples (ca. 25 cm^3) were held in a flow system comprising a glass reservoir, a peristaltic pump, Tygon tubing, and a 1-mm pathlength quartz flow cell, and they were flowed rapidly such that each pump-probe pulse pair encountered fresh sample [34]. Cellophane samples were held rigidly between two quartz microscope slides, and were mounted in a custom-designed sample translator that gave rapid translation while exploring a wide area of the ca. 1 cm × 2 cm sample [34]. The sample integrity was monitored by recording UV–visible absorption spectra before and after the TRVIS studies: the maximum absorbance loss was found to be ≤1% for all samples except Navy HEXL, which gave ca. 20% maximum absorbance loss in cellophane.

3. Results

3.1. Steady-state studies

The UV–visible absorption spectra of the dye samples are shown in Fig. 3. The spectra from aqueous solutions of the model dyes are similar, with strong bands at ca. 480 nm resulting in their orange colours (Fig. 3, top). The spectra from aqueous solutions of the com-

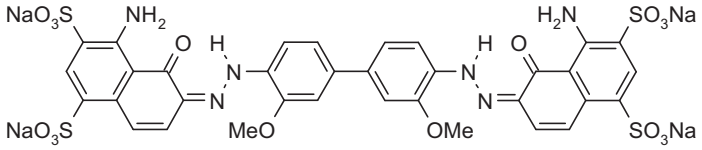

Direct Blue 1 (DB1)

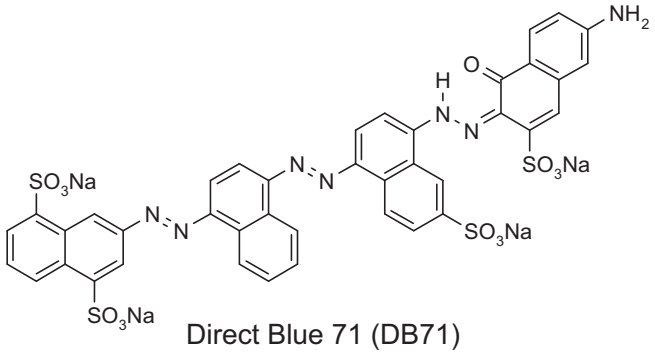

Direct Blue 71 (DB71)

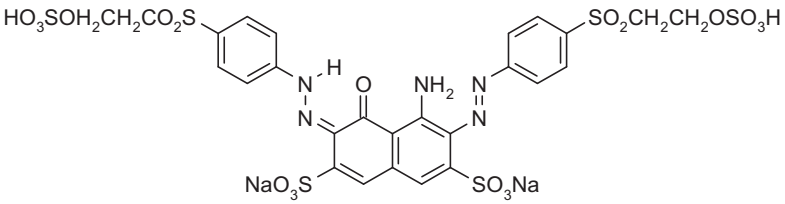

Reactive Black 5 (RB5)

Fig. 2. Structures of three of the commercial dyes.

mercial dyes are different from those of the model dyes but are generally similar to each other, with broad bands peaking at ca. 600 nm giving blue colours at these concentrations and the longer wavelengths resulting from increased conjugation. The samples were found to give only very weak emission, consistent with the literature on mono-azo/hydrazone dyes [24,26] and reported fluorescence quantum yields of $\leq 10^{-5}$ for DB1 and DB71 in water [35]. Absorption spectra recorded from the two commercial dyes deposited in cellophane are also shown in Fig. 3: the visible band of DB1 shows structure in cellophane that is not observed in aqueous solution and it is shifted to longer wavelength, with an additional peak at ca. 650 nm; the visible band of N-HEXL shows similar but more subtle changes, with an additional peak at ca. 630 nm on going from solution to cellophane.

3.2. Time-resolved studies

Time-resolved UV–visible absorption data are shown in Fig. 4, with values obtained from fitting the TRVIS kinetics given in Table 1. The TRVIS difference spectrum recorded 0.8 ps after 606 nm excitation of DB1 in aqueous solution was dominated by a very strong bleaching feature from the ground-state visible absorption band as shown in Fig. 4 (bottom left), and as typically reported for azo/hydrazone dyes [22,23,27]. The bleaching kinetics of DB1 are also shown in Fig. 4 (top right), and they fitted to an instrument-limited rise followed by a 4.0 ps single-exponential decay to an offset of 2% of the peak Δabsorbance that persisted to ≥1 ns (98% bleach recovery; Table 1); the much weaker transient absorption fitted to similar kinetics (Fig. 4, top right). The other four commercial dyes in aqueous solution showed slightly shorter lifetimes of ca. 1–2 ps and similar bleach recoveries on 606 nm excitation, whereas the model dyes showed comparable lifetimes of ca. 4 ps and slightly smaller bleach recoveries on 303 nm excitation. The kinetics shown by the two cellophane samples were different from those of the respective solutions. DB1 in cellophane showed a clear dual exponential decay that fitted to a ca. 2–3 ps component which was slightly faster than that in solution, and a longer-lived ca. 70–100 ps component of significant amplitude that decayed to a small offset. N-HEXL in cellophane showed a dominant ca. 1–2 ps component that was similar to that in solution, but its decay gave a bleach recovery by 20 ps that was clearly less than that in solution, and the data fitted to a second longer-lived component of small amplitude. Further studies showed that 303 nm excitation of DB1 and N-HEXL in solution and cellophane gave data similar to that recorded on 606 nm excitation. Steady-state UV–visible absorption spectra showed that the samples were essentially unchanged after the TRVIS experiments, with absorbance losses of typically

Table 1
Lifetimes (τ/ps) and relative bleaching amplitudes (A) from fits to the TRVIS kinetics shown in Fig. 4.[a]

Dye	Solution		Dye	Solution		Cellophane			
	τ	A		τ	A	τ_1	A_1	τ_2	A_2
M1	4.0	0.91	DB1	4.0	0.98	1.8	0.54	70	0.42
M2	4.2	0.81	DB71	1.8	0.99				
M3	4.3	0.91	RB5	1.4	0.98				
M4	3.7	0.95	N-HEXL	1.3	0.97	1.7	0.87	240	0.08
			NB-GG	1.8	0.98				

[a] Uncertainties of ca. ±0.3–0.8 ps and ±0.01–0.05 for solution τ and A, respectively.

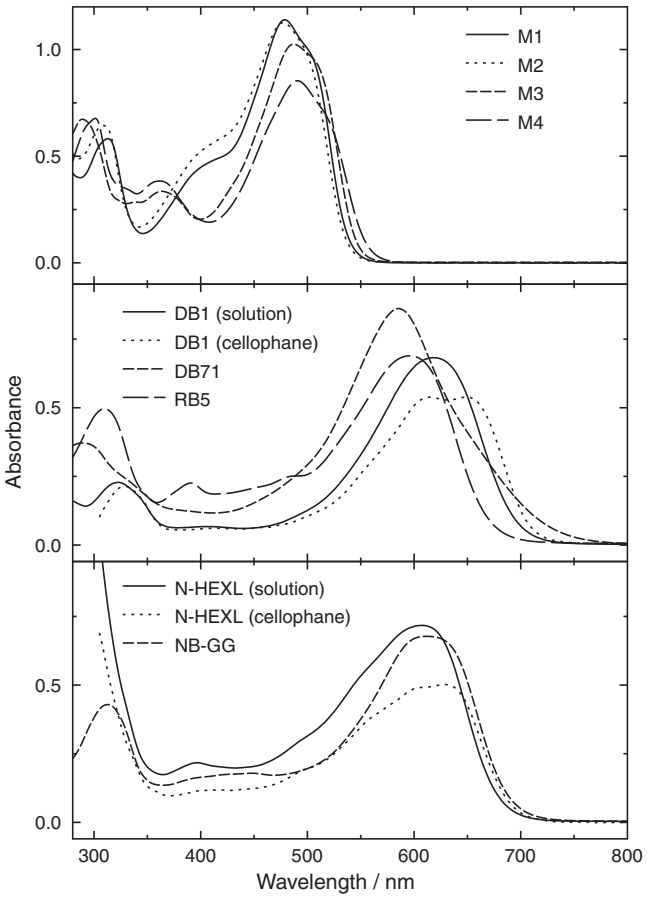

Fig. 3. Steady-state UV–visible absorption spectra of the samples: aqueous solutions in a 1 mm pathlength cell at concentrations of ca. 1–8 × 10^{-4} mol dm^{-3}; cellophane films of pathlength ca. 45 μm.

0–1% indicating low quantum yields for any photochemical reactions, consistent with our reported photofading quantum yields of ca. 10^{-7}, 10^{-6} and 10^{-5} for DB1 in solution, cellophane and cotton, respectively [2].

4. Discussion

4.1. Model dyes

Detailed studies reported previously on the model dyes M1–M4 [33] have shown that they occur as mixtures of azo and hydrazone tautomers in DMSO but predominantly as the hydrazone in water, that they aggregate at high concentrations in water but not in DMSO, and that they exhibit internal hydrogen bonding, all of which are typical effects observed for azo/hydrazone dyes [28–31]. Hence, our studies of M1–M4 in aqueous solution are on the hydrazone forms, as shown in Fig. 1. We estimate that M1–M4 were present mainly as monomers at the concentrations used here, based on the observed spectra versus those in the literature [31,33] and also on the reported dimerisation constant of Orange II [36,37], which is M1 without the sulfonate group on the naphthyl ring; M1 is likely to aggregate less readily than Orange II due to increased electrostatic repulsion from the additional sulfonate group. The ca. 4 ps bleach-recovery lifetimes and weak fluorescence from M1–M4 indicate that their excited singlet states decay predominantly by ultrafast non-radiative processes; excited-state tautomerisation and/or twisting at the azo/hydrazone group seem likely to provide rapid routes to non-radiative decay channels [24,25,27] that lead predominantly back to the starting hydrazone on relaxation to the ground state. Our time-dependent DFT calculations on Orange II have given electron redistributions for the lowest-lying hydrazone excited states that are different from those of the azo tautomer [31], suggesting that excitation of the M1–M4 hydrazones will, at least initially, populate a region of the excited-state potential-energy surface that is quite different from that accessed on excitation of the azo tautomers.

4.2. Commercial dyes

The commercial dye structures are more complicated than those of the model mono-azo dyes. Our studies of DB1 have shown that both halves of this bis-azo system occur in the hydrazone form in aqueous and non-aqueous (DMSO, DMF) solutions [28], as shown in Fig. 2, and that a mixture of monomers and dimers will be present at the concentration used here [29]. The ca. 4 ps bleach-recovery lifetime of DB1 is closely similar to those of the model dyes, suggesting that it may arise from similar non-radiative processes which are characteristic of broadly comparable hydrazone structures in aqueous solution. This tentative proposal is partially supported by time-dependent DFT calculations on DB1 [30] which have given a lowest-lying $\pi \rightarrow \pi^*$ transition with an electron redistribution pattern which is similar to that calculated for the lowest-lying $\pi \rightarrow \pi^*$ transition of the Orange II hydrazone [31], with both of these transitions having the largest visible-wavelength oscillator strengths for the respective dyes.

Of the other commercial dyes with known structures, DB71 has two azo groups that cannot tautomerise and a third that is likely to occur as the hydrazone, and RB5 has one azo group that may interact with an adjacent amine and a second that is likely to occur as the hydrazone. The ca. 1.5 ps bleach-recovery lifetimes of DB71 and RB5 are shorter than those of the pure hydrazone dyes (DB1 and M1–M4), suggesting that they may be characteristic of broadly comparable dyes containing a true azo group in aqueous solution. Excited-state tautomerisation and/or internal twisting again seem likely to provide rapid non-radiative routes leading predominantly back to the starting ground state but the shorter lifetimes suggest that the exact pathways differ and that the azo groups play a role, consistent with a report that azo tautomers have shorter excited-state lifetimes than hydrazones [27]. The bleach-recovery lifetimes of N-HEXL and NB-GG are similar to those of RB5 and DB71, suggesting that they may have structural similarities, such as an azo group, and similar excited-state decay mechanisms.

The changes in the steady-state UV–visible absorption spectra of DB1 and N-HEXL on cellophane deposition indicate that there is a change in their electronic structures. Our earlier UV–visible absorption, resonance Raman, and ^{1}H and ^{13}C NMR studies of DB1 in solution and in cellulose showed that the hydrazone form is retained on deposition from solution into cellophane and cotton [28]. Our detailed studies of concentration dependence showed that DB1 dimerises less readily in cellophane than in solution, due to relatively strong dye–cellulose interactions, and the measured dimerisation constant in cellophane [29] indicates that it will occur mainly as monomers at the concentration used here. We have suggested that changes in the UV–visible and Raman spectra of DB1 arise from changes in internal hydrogen bonding due to competitive interactions with cellulose, as well as other subtle structural changes that may arise from surface deposition and the move to a low-polarity environment [28].

It is established in the general literature on cellulose that the polysaccharide chains in cellophane and cotton are arranged into amorphous regions that contain considerable amounts of water giving a polar environment, and crystalline regions that are apolar [38–40]. Recent EPR studies with spin probes have shown that the behaviour of guest molecules in these nanoporous materials experience two major domains with different microviscosities aris-

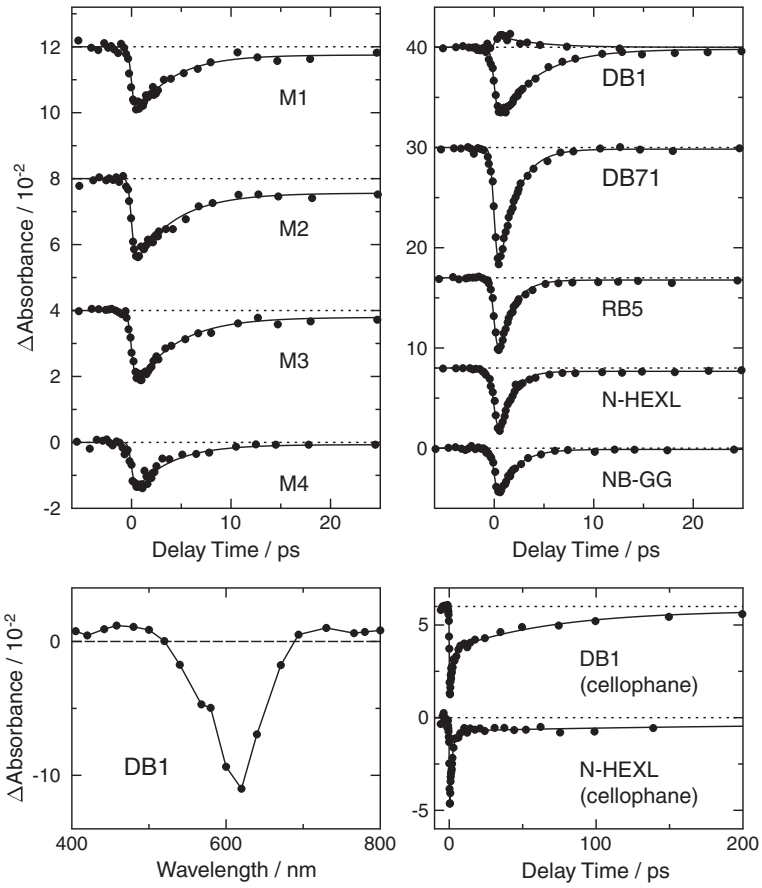

Fig. 4. TRVIS kinetics: model dyes pump 303 nm, probe ca. 500 nm (top left); commercial dyes pump 606 nm, probe 580 nm in solution (top right), with additional probe at 458 nm (transient absorption) shown for DB1; commercial dyes pump 606 nm, probe 640 nm in cellophane (bottom right); solid lines show fits, with traces offset for clarity. TRVIS spectrum of DB1 in solution: pump 606 nm, delay time 0.8 ps (bottom left).

ing from their presence in amorphous and apolar regions [41,42]. The bleach-recovery kinetics of DB1 in cellophane show a ca. 1.8 ps component that is slightly shorter than that in water, and a new ca. 70 ps component of comparable amplitude, and hence these two lifetimes may arise from DB1 in different regions of cellophane, with the short-lived component arising from DB1 in a liquid-like environment and the other component arising from DB1 in a more constrained environment giving a longer lifetime due to limited molecular flexibility. This effect is comparable to that observed on a similar timescale when Orange II binds to proteins and cyclodextrins [24,25]. Although the timescale and precise effects may differ, this observation is also comparable to our observation that the triplet excited state of a photoinitiator showed a single exponential decay in water and a dual exponential decay in cellophane [32] that we suggested may arise from some molecules being in the amorphous regions and others interacting with the surfaces of cellulose crystallites. The effects of cellophane deposition on N-HEXL are similar but less distinct than those on DB1, which may reflect different interactions with cellulose and different partitioning within the cellophane regions. Overall, these two dyes clearly have longer bleach-recovery lifetimes with slightly smaller amplitudes in cellophane than they do in solution.

5. Conclusions

Ultrafast time-resolved UV–visible absorption spectroscopy has shown that the direct photoexcitation of four model mono-azo dyes and five commercial azo dyes results in rapid and efficient ground-state recovery in ca. 1–5 ps in aqueous solution. Two commercial azo dyes deposited in cellophane have shown additional longer-lived components with >50 ps lifetimes and slightly smaller recovery amplitudes. Together, the observations indicate that rapid non-radiative decay dominates the primary excited-state dynamics of these dyes but suggest that subtle changes in the starting structures and excited-state potential-energy surfaces caused by intermolecular interactions with cellulose cause effects on the picosecond timescale that may be implicated in the commercially important photofading mechanisms of azo dyes on textile and other surfaces.

Acknowledgements

We acknowledge the support of Unilever Research.

References

[1] J. Oakes, Rev. Prog. Color. 31 (2001) 21–28.
[2] L.C. Abbott, P. MacFaul, L. Jansen, J. Oakes, J.R. Lindsay Smith, J.N. Moore, Dyes Pigments 48 (2001) 49–56.
[3] S.N. Batchelor, D. Carr, C.E. Coleman, L. Fairclough, A. Jarvis, Dyes Pigments 59 (2003) 269–275.
[4] T. Hihara, Y. Okada, Z. Morita, Dyes Pigments 60 (2004) 23–48.
[5] I.K. Lednev, T.-Q. Ye, R.E. Hester, J.N. Moore, J. Phys. Chem. 100 (1996) 13338–13341.
[6] I.K. Lednev, T.-Q. Ye, P. Matousek, M. Towrie, P. Foggi, F.V.R. Neuwahl, S. Umapathy, R.E. Hester, J.N. Moore, Chem. Phys. Lett. 290 (1998) 68–74.
[7] I.K. Lednev, T.-Q. Ye, L.C. Abbott, R.E. Hester, J.N. Moore, J. Phys. Chem. A 102 (1998) 9161–9166.
[8] P.D. Chowdary, S. Umapathy, J. Raman Spectrosc. 39 (2008) 1538–1555.
[9] C.M. Stuart, R.R. Frontiera, R.A. Mathies, J. Phys. Chem. A 111 (2007) 12072–12080.
[10] H. Satzger, C. Root, M. Braun, J. Phys. Chem. A 108 (2004) 6265–6271.

[11] T. Fujino, S.Y. Arzhantsev, T. Tahara, Bull. Chem. Soc. Jpn. 75 (2002) 1031–1040.
[12] H. Zollinger, Color Chemistry, 3rd ed., Wiley-VCH, Weinheim, 2003.
[13] L.M.G. Jansen, I.P. Wilkes, F. Wilkinson, D.R. Worrall, J. Photochem. Photobiol. A 125 (1999) 99–106.
[14] F. Ruyffelaere, V. Nardello, R. Schmidt, J.-M. Aubry, J. Photochem. Photobiol. A 183 (2006) 98–105.
[15] K.K. Sharma, B.S.M. Rao, H. Mohan, J.P. Mittal, J. Oakes, P. O'Neill, J. Phys. Chem. A 106 (2002) 2915–2923.
[16] K.K. Sharma, P. O'Neill, J. Oakes, S.N. Batchelor, B.S.M. Rao, J. Phys. Chem. A 107 (2003) 7619–7628.
[17] P. Yadav, B.S.M. Rao, S.N. Batchelor, P. O'Neill, J. Phys. Chem. A 109 (2005) 2039–2042.
[18] P. Hunt, D.R. Worrall, F. Wilkinson, S.N. Batchelor, J. Am. Chem. Soc. 124 (2002) 8532–8533.
[19] P. Hunt, D.R. Worrall, F. Wilkinson, S.N. Batchelor, Photochem. Photobiol. Sci. 2 (2003) 518–523.
[20] V. Nadtochenko, J. Kiwi, J. Chem. Soc., Faraday Trans. 93 (1997) 2373–2378.
[21] J. Bandara, J. Kiwi, New J. Chem. 23 (1999) 717–724.
[22] K. Vinodgopal, P.V. Kamat, J. Photochem. Photobiol. A 83 (1994) 141–146.
[23] C. Nasr, K. Vinodgopal, S. Hotchandani, A.K. Chattopadhyay, P.V. Kamat, Radiat. Phys. Chem. 49 (1997) 159–166.
[24] A. Douhal, M. Sanz, L. Tormo, Proc. Natl. Acad. Sci. U.S.A. 102 (2005) 18807–18812.
[25] H. Yui, M. Takei, Y. Hirose, T. Sawada, Rev. Sci. Instrum. 74 (2003) 907–909.
[26] T. Susdorf, A.K. Bansal, A. Penzkofer, S.-L. Guo, J.-M. Shi, Chem. Phys. 333 (2007) 49–56.
[27] R. Karpicz, V. Gulbinas, A. Stanishauskaite, A. Undzenas, Chem. Phys. 269 (2001) 357–366.
[28] L.C. Abbott, S.N. Batchelor, L. Jansen, J. Oakes, J.R. Lindsay Smith, J.N. Moore, New J. Chem. 28 (2004) 815–821.
[29] L.C. Abbott, S.N. Batchelor, J. Oakes, J.R. Lindsay Smith, J.N. Moore, J. Phys. Chem. B 108 (2004) 13726–13735.
[30] L.C. Abbott, S.N. Batchelor, J. Oakes, J.R. Lindsay Smith, J.N. Moore, J. Phys. Chem. A 108 (2004) 10208–10218.
[31] L.C. Abbott, S.N. Batchelor, J. Oakes, B.C. Gilbert, A.C. Whitwood, J.R. Lindsay Smith, J.N. Moore, J. Phys. Chem. A 109 (2005) 2894–2905.
[32] L.C. Abbott, S.N. Batchelor, J.R. Lindsay Smith, J.N. Moore, J. Phys. Chem. A 113 (2009) 6091–6103.
[33] J. Oakes, P. Gratton, R. Clark, I. Wilkes, J. Chem. Soc., Perkin Trans. 2 (1998) 2569–2575.
[34] T.-Q. Ye, C.J. Arnold, D.I. Pattison, C.L. Anderton, D. Dukic, R.N. Perutz, R.E. Hester, J.N. Moore, Appl. Spectrosc. 50 (1996) 597–607.
[35] S.J. Isak, E.M. Eyring, J.D. Spikes, P.A. Meekins, J. Photochem. Photobiol. A 124 (2000) 77–85.
[36] R.L. Reeves, M.S. Maggio, S.A. Harkway, J. Phys. Chem. 83 (1979) 2359–2368.
[37] T. Asakura, M. Ishida, J. Colloid Interface Sci. 130 (1989) 184–189.
[38] H.A. Krässig, Cellulose, Gordon Breach Science Publishers, Amsterdam, 1993.
[39] D. Klemm, B. Phillip, T. Heinze, U. Heinze, W. Wagenknecht, Comprehensive Cellulose Chemistry, vol. 1, Wiley-VCH, Weinheim, 1998.
[40] J. Shore (Ed.), Cellulosics Dyeing, Society of Dyers and Colourists, Bradford, 1995.
[41] S. Frantz, G.A. Hübner, O. Wendland, E. Roduner, C. Mariani, M.F. Ottaviani, S.N. Batchelor, J. Phys. Chem. B 109 (2005) 11572–11579.
[42] S. Frantz, O. Wendland, E. Roduner, C.J. Whiteoak, S.N. Batchelor, J. Phys. Chem. C 111 (2007) 14514–14520.